A Novel Approach to Extract Colon Lumen from CT Images for Virtual Colonoscopy

Dongqing Chen*, *Member, IEEE*, Zhengrong Liang, *Member, IEEE*, Mark R. Wax, Lihong Li, *Student Member, IEEE*, Bin Li, and Arie E. Kaufman, *Member, IEEE*

***Abstract*—An automatic method has been developed for segmentation of abdominal computed tomography (CT) images for virtual colonoscopy obtained after a bowel preparation of a low-residue diet with ingested contrast solutions to enhance the image intensities of residual colonic materials. Removal of the enhanced materials was performed electronically by a computer algorithm. The method is a multistage approach that employs a modified self-adaptive on-line vector quantization technique for a low-level image classification and utilizes a region-growing strategy for a high-level feature extraction. The low-level classification labels each voxel based on statistical analysis of its three-dimensional intensity vectors consisting of nearby voxels. The high-level processing extracts the labeled stool, fluid and air voxels within the colon, and eliminates bone and lung voxels which have similar image intensities as the enhanced materials and air, but are physically separated from the colon. This method was evaluated by volunteer studies based on both objective and subjective criteria. The validation demonstrated that the method has a high reproducibility and repeatability and a small error due to partial volume effect. As a result of this electronic colon cleansing, routine physical bowel cleansing prior to virtual colonoscopy may not be necessary.**

***Index Terms*—Bowel preparation, electronic colon cleansing, image segmentation, virtual colonoscopy.**

I. Introduction

COLORECTAL carcinoma is the second leading cause of cancer-related deaths in the United States with 56 000 deaths reported in 1998 and an estimated 131 600 new cases were diagnosed [20]. Colonic polyps that are 10 mm or larger in diameter are considered to be clinically significant, since they have a high probability of being malignant [15]. Detection and removal of smaller sized polyps can eliminate over 90% of colon cancer cases.

Currently available colorectal cancer screening procedures include digital rectal examination, fecal occult blood test, flexible sigmoidoscopy, barium enema, and optical colonoscopy. These diagnostic tests differ greatly with respect to safety, ease of performance, degree of patient compliance, expense, and diagnostic accuracy. Among these methods, only optical colonoscopy and barium enema might be able to examine the entire colon. Optical colonoscopy requires intravenous sedation, takes approximately one hour to perform, has difficulty in examing the cecum, the most distal portion, and is expensive. Barium enema requires a great deal of patient physical cooperation to obtain X-rays at different views, and has a low sensitivity. In recent years, virtual colonoscopy technology has been developed as an alternative method of massive population screening for examining the entire colon for early cancer detection [6], [7], [11], [13], [14], [18]. This technology uses a computer system to navigate through the colon model reconstructed from the patient's abdominal CT images. It has been shown that this technology is effective in imaging colonic polyps as small as 3 mm in diameter [8].

All techniques that examine the colon require a clean lumen, eliminating residual materials that can falsely be interpreted as colonic masses. Prior to any of these examinations, patients undergo a bowel cleansing preparation which includes either washing the colon with a large amount of liquids or administering medications and enemas to induce bowel movements [7], [18]. This bowel preparation is often more unpleasant than the examination itself. An alternative method of cleansing the colon would be very attractive. In virtual colonoscopy, contrast solutions can be ingested to enhance the image intensities of the stool and fluid. By applying image segmentation algorithms, these colonic materials can be virtually removed from the images without the patient undergoing physical bowel washing. This paper will focus on the development of an automatic segmentation method to remove the contrasted colonic materials for virtual colonoscopy.

II. Methods and Materials

A. Bowel Preparation and Imaging Protocol

Five volunteers were recruited for this study with written consents. Some of these subjects were used as training samples for validating the hypothesis of the method and all of them were used for evaluating the performance of the method. The training samples were chosen for an equal distribution in gender with a wide age range, see Table I, where three patients were added to include variation in a large population. All volunteers had the following bowel preparation. During the day prior to CT scan, the volunteers took a high fluid, low residue diet for the meals. In order to enhance residual colonic materials, they ingested contrast solutions of 250 cc barium sulfate suspension (2.1% w/v,

Manuscript received May 4, 1999; revised August 18, 2000. This work was supported by the National Institutes of Health (NIH) under Grant CA79180 of the National Cancer Institute; Grant HL54166 of the National Heart, Lung and Blood Institute; Grant NS33853 of the National Institute of Neurological Disorder and Stroke; and Established Investigator Award of the American Heart Association. The Associate EWditor responsible for coordinating the review of this paper and recommending its publication was W. Higgins. *Asterisk indicates correspondintg author.*

*D. Chen is with the Departments of Radiology, State University of New York, Stony Brook, NY 11794 USA (e-mail: dchen@clio.rad.sunysb.edu.).

Z. Liang, M. R. Max, L. Li, B. Li, and A. E. Kaufman are with the Departments of Radiology and Computer Science, State University of New York, Stony Brook, NY 11794 USA.

Publisher Item Identifier S 0278-0062(00)10613-5.

TABLE I
SUBJECT INFORMATION, WHERE F AND M STAND FOR THE FEMALE AND MALE, AND V AND P FOR THE VOLUNTEER AND PATIENT

Group	Training group						Testing group	
Gender	F	F	M	M	M	F	M	M
Age	21	23	41	44	58	70	25	28
Type	V	V	P	P	V	P	V	V
Number	1	2	3	4	5	6	7	8

E-Z-EM, Inc.) with each meal and 120 ml of MD-Gastroview (diatriuzoate meglumine and diatriozoate sodium solutions) in equal 60 ml amounts during the evening and in the morning before the CT scan. All patients used the same bowel preparation with addition of magnesium citrate laxative and bisacodyl tablets and suppository for physical colon cleansing.

Prior to acquiring CT images, 1.0 mg of Glucagon was given intravenously in order to reduce colonic motion and spasm, followed by introducing approximately 1000 cc of CO_2 through a small bore rectal tube to inflate the colon. All CT images were acquired in less than 40 s during a single breath hold. Using a GE/CTI spiral CT scanner, 5mm collimation with pitch between 1.5–2.0 : 1, depending upon the span of the colon as determined from a digital scout radiograph, was performed. Scan parameters included 120 kVp, 180–280 mA (lower mA for volunteers) and field of view (FOV) between 34–40 cm based on the abdominal size. The acquired data were reconstructed at 1-mm intervals with a 512 $\times$ 512 array, resulting in 300–450 slices for each dataset. Both supine and prone positions were scanned for validation purpose. For the same purpose, each volunteer was also scanned in the following day after the first CT scan and a day of low-residue diet, resulting in four datasets.

B. Feature Analysis of Image Data

To minimize computing time, the voxels outside the body contour were first eliminated. The remaining is called body voxels. This was achieved by a boundary-search algorithm [9]. Similar to Markov random field (MRF) models [5], [9], [12], [19], we assume that a three–dimensional (3-D) object of a similar tissue type in a CT image should be in a contiguous 3-D volume, naturally including partial volume effect. It is reasonable to classify the body voxels based on the intensity similarity within certain spatial range. The diameter of the local range for a given voxel should be less than 5 mm considering the partial volume effect and the 5-mm-thick collimation. By the acquisition protocol described above, each voxel was 1 mm thick with size in the x–y axial plane varying from 0.64 to 0.94 mm depending on the FOV. The chosen local volume is depicted in Fig. 1. Its diameter is less than 4.6 mm in all directions. The intensities of those 23 voxels in a local volume form a twenty–three dimensional (23-D) local intensity vector. The goal of the low-level processing is to classify the body voxels based on their local intensity vectors.

Each dataset consists of millions of body voxels, where each voxel has a 23-D local intensity vector. This requires intensive computational effort to manipulate such a large quantity of vectors. To reduce the computing burden, a feature analysis of the local vector series is necessary [3]. The principal component analysis (PCA) [1] was then applied to the local vector series to determine the dimension of the feature vectors and the associated orthogonal transformation matrix [i.e., the Karhunen–Loeve (K–L) transformation matrix]. The PCA on the datasets of the training samples showed that a reasonable dimension of the feature vectors was 5, where the summation of the first five principal components' variances was more than 92% of the total variance.

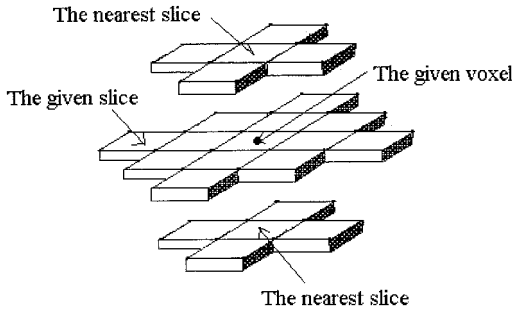

Fig. 1. Depiction of the local volume for a voxel.

It is computationally costly to determine K–L matrix for each dataset. A general K–L matrix was then determined by the training samples and used for segmenting all datasets acquired from the same source, i.e., from the same scanner with the same imaging protocol described previously. To provide evidence for using the general K–L matrix for all datasets acquired from the same source, the Kolomogorve–Smirnov test was performed [16], which aims to prove that all datasets from the same source could be regarded as a sample set from an identical probability distribution. A supine dataset was chosen from each of the training samples. The associated cumulative distribution function (CDF) was obtained and denoted by $S_k(x), k = 1, 2, \ldots, 8$ (some volunteers have two supine scans acquired in two consecutive days). By utilizing all datasets (both supine and prone) in the training samples, a general CDF, denoted by $\overline{S}(x)$, was also computed. This $\overline{S}(x)$ was regarded as the estimation of the source CDF. Then, the hypothesis H0: *$S_k(x)$ and $\overline{S}(x)$ are identical distributions* may be tested against hypothesis H1: *$S_k(x)$ and $\overline{S}(x)$ are not identical*, for $k = 1, 2, \ldots, 8$. The differences of greatest magnitude $D(k) \equiv \max_x |S_k(x) - \overline{S}(x)|$ were listed in Table II.

The table [17, Table VIII] gives the critical value with a two-tail test at a nominal 1% significance level of 0.45. All differences listed in Table II are less than 0.45 (the largest sample size in[17, Table VIII] is 20, where the critical value is associated to this sample size). Hence, we accept H0, i.e., all datasets can be regarded as coming from an identical probability distribution. Therefore, the general K–L matrix determined by the training samples can be applied to segment all the datasets acquired using the same scanning protocol.

C. Vector Quantization Algorithm

For the low-level classification, the K–L transformation was first applied to the local vector series. In the K–L domain, the feature vectors were formed by the first five principal components from the transformed vector series. Then, the feature vectors were classified into several classes. There are several approaches to classify the vectors [4]. In general, an automated

TABLE II
THE GREATEST MAGNITUDES OF THE DIFFERENCE BETWEEN THE SUBJECTS= CDF AND THE SOURCE CDF

	1	2	3	4	5	6	7	8
D(k)	0.2361	0.1191	0.0459	0.10605	0.1243	0.0635	0.0812	0.0601

algorithm is desired, i.e., an unsupervised self-adaptive vector quantization (VQ) algorithm is a candidate. A self-adaptive on-line VQ algorithm was developed and is presented below. Let X_i, $i = 1, 2, \ldots, N$, be the feature vector series, where N is the number of feature vectors; K denote the maximum number of classes; and T be a threshold for vector similarity. The VQ algorithm generates a representative vector a_k for each class. Let n_k be the number of feature vectors in the kth class after classification.

The algorithm is outlined as follows.

```
1) Set a_1 = X_1, n_1 = 1, and K̂ = 1;
2) Obtain the class number K̂ and class
  parameters (a_k, n_k), k = 1, 2, ..., K.
  For (i = 1; i <= N; i++) {
    For (j = 1; j < K̂; j++) {
      Calculate d_j = dist(X_i, a_j);
    }
    δ = arcmin_j(d_j);
    If ((d_δ < T) or (K̂ = K)) {
    Update the representative vector of
  the δth class:
      a_δ = (n_δ · a_δ + X_i)/(n_δ + 1); n_δ = n_δ + 1;
    }
Else{ Generate a new class
      K̂ = K̂ + 1; a_K̂ = X_i; n_K̂ = 1;
    }
  }
3) Label each feature vector to a class
  according to the nearest neighbor rule
  For (i = 1; i <= N; i++) {
    For (j = 1; j < K̂; j++) {
      Calculate d_j = dist(X_i, a_j);
    }
    δ = arcmin_j(d_j);
    Label voxel i to the δth class;
  }
```

where $dist(x, y)$ is the Euclidean distance between x and y, and $arc\min_j(d_j)$ gives the integer j which realizes the minimum value of d_j.

The class number and the representative vector for each class can be obtained in a single scan on all feature vectors. This reduces greatly the computing time as compared to iterative VQ algorithms, e.g., the LBG algorithm [10]. The representative vector of each class is an estimation of the mean vector of that class. From the central limit theorem [2], the larger the number in a class is, the more accurate the representative vector estimates the mean vector of that class. For a colon dataset, there are millions of body voxels. Hence, the representative vector is a good estimation to the mean of that class [2].

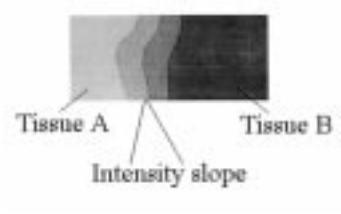

Fig. 2. An example showing the intensity value change gradually from tissue A to tissue B. The overlap area represents the partial volume region.

The algorithm is similar to an unsupervised clustering algorithm. The number of classes and the representative vectors are updated continuously when more vectors are included in the calculation. From this point, the algorithm can be regarded as a learning procedure. It depends only on two parameters: $\mathbf{K}$ the upper bound of possible classes and $\mathbf{T}$ the vector similarity threshold. In abdominal CT images, there are roughly four classes that can be perceived based on their intensity features: 1) air, 2) soft tissue, 3) muscle, and 4) bone or the enhanced residual materials. The intensity values of these four classes increase from the lowest to the highest. Due to partial volume effect, there exists an intensity slope between two spatially contiguous tissue areas (see Fig. 2). The voxels in this slope-area are called partial volume voxels. To mitigate the under or over estimation of tissue boundary, it is reasonable to find the tissue boundary within the slope-area rather than on the edge of the slope-area. In other words, the partial volume area should be divided into two subareas. The left partial volume class is called partial volume from A to B and the right one is called partial volume from B to A. The partial volume area from A to B is labeled as tissue A and the partial volume area from B to A is labeled as tissue B in this study. In the CT images, there are two kinds of voxels within the colon lumen: 1) air and 2) enhanced materials. Each kind has a partial volume overlap to area of soft tissue/muscle. Assigning two partial volume classes to each of the overlap areas results in four partial volume classes in total. Therefore, the maximum class number $\mathbf{K}$ for the classification algorithm was set to eight in this study. $\mathbf{T}$ is more crucial to the classification than $\mathbf{K}$. If it is too large, only one class could be obtained. If it is too small, redundant classes may occur. According to our numerical experiments, $\mathbf{T}$ was set to the square root of the maximum component variance of the feature vector series. This allows the VQ algorithm to achieve the minimum class number with the maximum variance. Since T is estimated from the data, the algorithm is self-adaptive.

D. Extraction of the Colon Lumen

The results of the low-level classification were represented as a labeled image with integer values. The colon lumen consisted of four kinds of labeled voxels: 1) air, 2) partial volume from air to soft tissue/muscle, 3) enhanced materials, and 4) partial volume from enhanced materials to soft tissue/muscle.

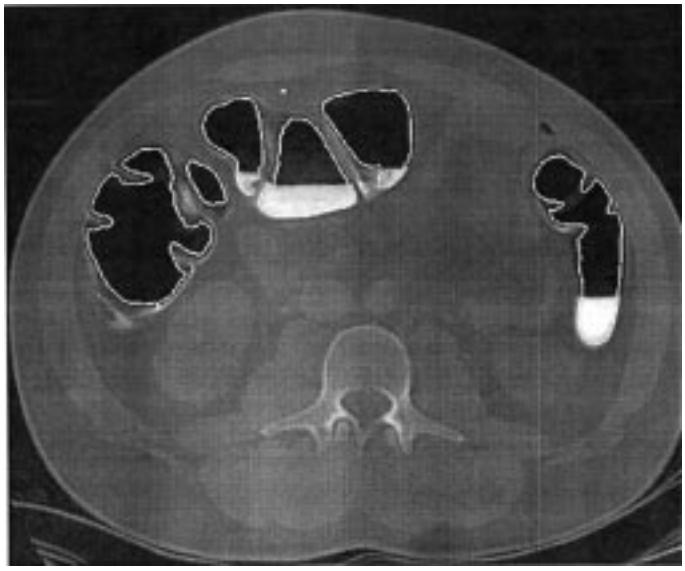

Fig. 3. A CT slice image and the delineated contour of colon lumen.

These four classes were denoted by 1, 2, 3, and 4, respectively. By applying the inverse K–L transformation to the class representative vectors, the intensities in the original image space for each class were obtained. Classes 1 and 3 were easily segmented since their intensities were the lowest and the highest, respectively. Since class 1 includes voxels of lung and class 3 includes voxels of bone and these voxels are not physically associated with the colon lumen, we can use region-growing strategies to remove the non colon-lumen voxels from classes 1 and 3. This is the high-level processing.

We removed lung voxels first. The regions of lungs are two contiguous 3-D volume on the left and right sides of the chest. If FOV covers the entire colon, air voxels in the top slice must be lung voxels. Two air voxels for both left and right lungs were determined as seeds for growing out the entire lung volume by using a region-growing algorithm. After removing the lung volume, the remained voxels in class 1 were inside the colon lumen. Given the air lumen, the partial volume voxels of class 2 from air to soft tissue/muscle were then determined because they were contiguous to the air lumen in both geometry space and intensity feature.

Assuming that bone is separated from colon lumen, the voxels of enhanced materials were then determined from class 3 by a seed in the lumen with the region-growing algorithm. If a voxel belonged to class 3 and there existed at least one voxel of air in the lumen which was 2.5 mm or less away from the given voxel, it was a seed for growing out the volume of the enhanced materials. The partial volume voxels of class 4 from enhanced materials to the soft tissue/muscle were determined by finding the class closest to the material class in both geometry space and intensity feature. Given the four classes of voxels representing the colon lumen, the last task was to label the boundary voxels between air and enhanced materials in the image space. The enhanced material forms a basin-like volume with a flat surface due to the gravitation [9]. This surface was the boundary between air and enhanced material, and was found by sending a ray from an air voxel and examining whether the ray reaches an enhanced voxel within 2 mm.

E. Evaluation Method

Optical colonoscopy is currently utilized as the gold standard for validating virtual colonoscopy methods for detecting colonic polyps of 5 mm or larger in diameter. For the electronic cleansing without physical bowel washing, the gold standard is not applicable. Instead, we acquired both supine and prone scans for each subject and furthermore repeated the scans on the next day for the volunteers, aiming to measure the reproducibility, repeatability and robustness on partial volume effect of the presented electronic cleansing technique. The results were subjectively judged by an experienced radiologist. Four objective parameters were calculated from the results to indirectly measure the performance. The first two were used to measure the segmentation error created by partial volume effect. The other two were used to demonstrate reproducibility (by the same dataset) and repeatability (by both supine and prone scans of the same subject) of the method. All these four parameters were calculated from the extracted colon lumen.

1) Average thickness of the partial volume layer (ATPV): This is the average thickness in 3-D space of the partial volume layer from both air and enhanced materials to soft tissue/muscle. If this parameter is larger than 5 mm, then polyps of 5 mm in diameter may not be accurately detected.
2) Partial volume percentage (PVP): PVP $=$ (summation of the volume of partial volume layer from air to soft tissue/muscle and the volume of partial volume layer from enhanced materials to soft tissue/muscle)/(the volume of entire extracted colon lumen).

   The volume was counted by the number of voxels in the region. This parameter estimates the ratio of the partial volume voxels to the entire colon lumen.
3) Mean intensities of the air lumen (AL) and the enhanced materials (ERM) voxels. The intensity is in HU.
4) $Diff(\alpha) = (|\alpha_s - \alpha_p|/\alpha_s) \times 100\%$, where α_s is one of the parameter defined previously for the supine dataset and α_p is one corresponding to the prone dataset acquired from the same subject on the same day. The definition applies to the two-day scans. A smaller value $Diff(a)$ reflects a better reproducibility or repeatability.

III. Results and Discussion

For subjects 3, 4, and 6, only supine scan was acquired (Table I). For subjects 1, 2, 5, and 7, both supine and prone scans were acquired on two consecutive days. Subject 8 was scanned in the supine position on two consecutive days. There was a total of 21 datasets, 13 in supine position and eight in prone position. The 15 datasets in the training samples were used to determine the size of the feature vectors and the general K–L matrix. It took nearly 6 hours to generate the K–L matrix. This matrix was then applied to segment all the 21 datasets. Fig. 3 shows a CT slice image and the extracted lumen contour within the CT image. Fig. 4 depicts the removed enhanced materials in 3-D. Fig. 5(a) displays the outside view of the entire extracted colon

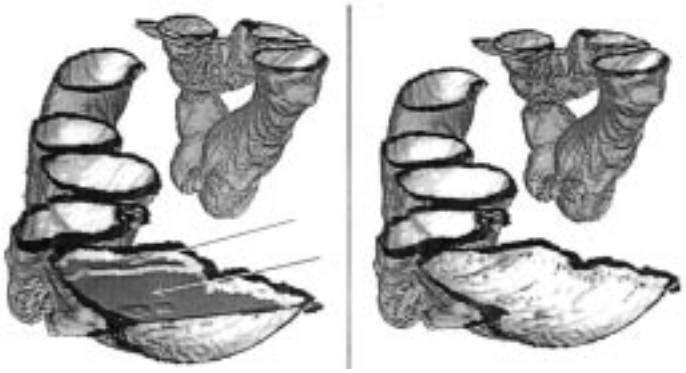

Fig. 4. Demonstration of removal of enhanced material (arrows).

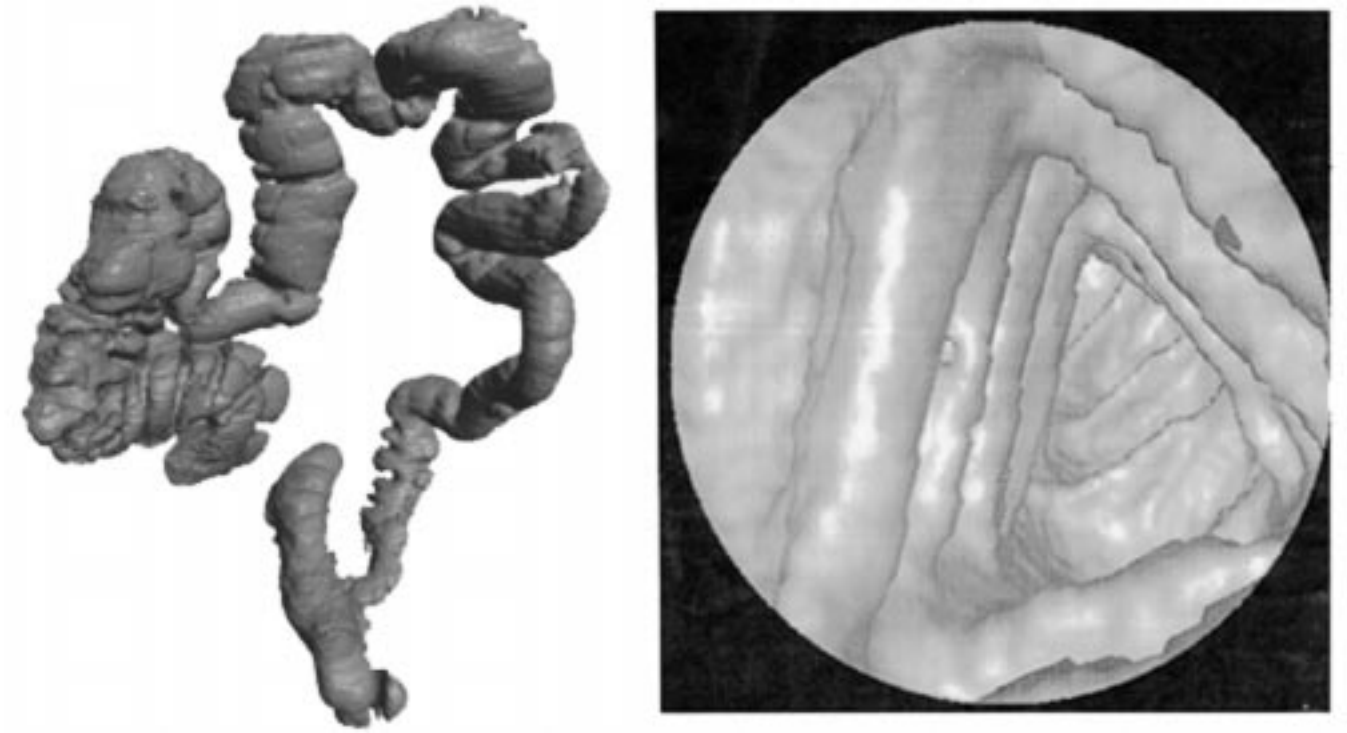

(a) (b)

Fig. 5. The overview of the entire colon lumen (a) and the inside view of a segment of colon lumen (b).

lumen and Fig. 5(b) shows the inside view of a colon segment. These figures were generated from subject 8. The segmentation of the colon lumen took less than 9 minutes on a SGI/Octane desktop workstation with dual CPU's of R10000, 250 MHz, and 890 MB RAM. No parallel implementation was utilized. Since we did not utilize seeded region-growing technique to grow out the lumen, our method was able to delineate all segments of the entire colon lumen when collapses presented.

A. Subjective Evaluation

The radiologist examined the segmentation results and was satisfied. The entire lumens from 13 datasets of subjects 2, 3, 4, 5, 6, and 8 were successfully delineated, where four datasets showed colon collapses. The enhanced materials were removed satisfactorily. Although some small artifacts remained on the wall surface near the boundary between air and enhanced material, these were smaller than 5 mm and were not clinically significant. In one subject, at some locations, the small bowel adjacent to the colon, appeared "attached" to the colon lumen. For example, subject 1 did not follow the diet instruction, eating a big breakfast on the first day prior to CT scan, which resulted in the stomach and small bowel filled with enhanced materials. The extracted lumen included part of the stomach and several small bowel segments. (In the second day after correcting the error, the colon lumen was successfully extracted). For subject 7, due to a 5-mm thickness collimation, some boundary areas between the lungs and colon were not resolved, resulted in connection of lungs and colon lumen. The algorithm could still remove the enhanced materials and extracted the lumen including part of the lungs. (A smaller slice collimation in data acquisition is recommended). Excluding the two

TABLE III
PARTIAL VOLUME ERROR ESTIMATION

		ATPV (mm)	Mean Intensity (HU)		PVP
			AL	ERM	
S1	Supine	2.06	-888	857	4.9%
	Prone	1.89	-887	812	5.0%
S2	Supine	2.38	-905	891	9.2%
	Prone	2.57	-897	847	9.8%
S8	Supine	2.17	-906	872	6.9%
	Prone	2.09	-901	908	7.1%

TABLE IV
REPEATABILITY TEST

	Diff(.)			
	ATPV	AL	ERM	PVP
S1	8.3%	0.11%	5.25%	2%
S2	8.0%	0.9%	4.9%	6.5%
S8	3.7%	0.6%	4.1%	2.8%

datasets of subject 1 and four datasets of subject 7 from the total 21 datasets, 15 lumens were successfully delineated and were inspected using our developed virtual colonoscopy system [7], [8]. The attached areas between colon and small bowel, as well as between colon and lungs, were deleted manually before navigating through the colon lumens. The navigations through both supine and prone scans, as well as the second day scans of each subject agreed each other, i.e., they agreed with the assumed gold standard that the young volunteers have no polyps.

B. Objective Evaluation

The supine and prone datasets acquired on the same day from subjects 1, 2, and 8, respectively, were used to compute the parameters for repeatability test and partial volume effect measurement. The results are listed in Tables III and IV, where S# means subject #. The reproducibility test from the same dataset was excellent, because of the fully automated process.

C. Discussion

If the bowel preparation instruction was followed, as most subjects did, the segmentation results were satisfactory. The enhanced colonic materials were removed successfully except for some small artifacts near the area where air, colon wall, and enhanced material connected. These artifacts form a small artificial horizontal ring on the colon wall surface that can be easily distinguished from the colonic folds. Nevertheless, if a polyp smaller than 5 mm is located on the ring, it could potentially be missed in the virtual colonoscopy examination. Further research is needed to minimize these artifacts for detecting smaller polyps. If a segment of small bowel touches the colon and is filled with the enhanced materials, this segment may be delineated with a higher probability as the colon lumen. This can be avoided by not eating any food/drink in the morning prior to CT scan. Another possible solution is to use an interactive display tool to manually correct the touched segment. The attachment of the lungs to colon lumen can be avoided with a higher axial resolution. This may be achieved by a multidetector ring CT system.

In our algorithm, the colon lumen is delineated by removing the volume which is not associated with the colon lumen, rather than finding some seeds of the colon lumen to grow out the entire lumen. This ensures that the entire colon lumen could be delineated even if there are collapsed segments. This is a very attractive advantage considering that the colon collapse happens frequently.

The partial volume effect was considered in our algorithm. The average partial volume layer shown in Table III is 2.57 mm or less in thickness. This ensures that polyps of 5 mm or larger in diameter cannot be affected by the partial volume effect within the extracted colon lumen. However, some of the flat polyps could be missed.

All the parameter differences in Table IV are less than 8.3% and most of them are less than 6.5%, demonstrating good repeatability of our method. This statement concurs with the subjective evaluation.

D. Conclusion

Our two-stage segmentation method designed for the bowel preparation using a low-residue diet with ingested colonic contrast solutions was computational efficiency and showed satisfactory performance. Since the training samples include patient datasets, the segmentation method is applicable to both cases with and without additional physical bowel cleansing. Most importantly, the electronic colon cleansing technique demonstrated the feasibility of performing virtual colonoscopy without the need for pre-procedure physical bowel cleansing.

ACKNOWLEDGMENT

The authors greatly appreciate the valuable comments on K–S test from Dr. S. Li.

REFERENCES

[1] C. Chatfield and A. J. Collins, *Introduction to Multivariate Analysis.* London, U.K.: Chapman & Hall, 1980.

[2] W. Feller, *An Introduction to Probability Theory and its Applications*, 3rd ed. New York: Wiley, 1968.
[3] K. Fukunaga, *Introduction to Statistical Pattern Recognition*, 2nd ed. New York: Academic, 1990.
[4] A. Gersho and R. M. Gray, *Vector Quantization and Signal Compression*. Boston, MA: Kluwer, 1992.
[5] S. Geman and D. Geman, "Stochastic relaxiation, Gibbs distributions, and the Bayesian restoration of images," *IEEE Trans. Pattern Anal. Machine Intell.*, vol. 6, pp. 721–741, 1984.
[6] A. Hara, C. Johnson, J. Reed, D. Ahlquist, H. Nelson, R. Ehman, C. McCollough, and D. Ilstrup, "Detection of Colorectal Polyps by CT Colography: Feasibility of a novel technique," *Gastroenterology*, vol. 110, pp. 284–290, 1996.
[7] L. Hong, A. Kaufman, Y.-C. Wei, A. Viswambharan, M. Wax, and Z. Liang, "3-D virtual colonoscopy," in *Proc. Biomedical Visualization*, M. Loew and N. Gershon, Eds., Atlanta, GA, 1995, pp. 26–33.
[8] L. Hong, Z. Liang, A. Viswambharan, A. Kaufman, and M. Wax, "Reconstruction and visualization of 3-D models of colonic surface," *IEEE Trans. Nucl. Sci.*, vol. 44, pp. 1297–1302, 1997.
[9] Z. Liang, F. Yang, M. Wax, J. Li, J. You, A. Kaufman, L. Hong, H. Li, and A. Viswambharan, "Inclusion of a priori information in segmentation of colon lumen for 3-D virtual colonoscapy," in *Conf. Rec. IEEE NSS-MIC*, Albuquerque, NM, Nov. 1997.
[10] Y. Linde, A. Buzo, and R. M. Gray, "An algorithm for vector quantizer designed," *IEEE Trans. Commun.*, vol. 28, pp. 84–95, 1980.
[11] E. McFarland, J. Brink, J. Loh, G. Wang, V. Argiro, D. Balfe, J. Heiken, and M. Vannier, "Visualization of colorectal polyps with spiral CT colography: Evaluation of processing parameters with perspective volume rendering," *Radiology*, vol. 205, pp. 701–707, 1997.
[12] T. N. Papps, "An adaptive clustering algorithm for image segmentation," *IEEE Trans. Signal Processing*, vol. 40, pp. 901–914, 1992.
[13] T. Parkins, "Computer lets doctors fly through the virtual colon," *JNCI*, vol. 86, pp. 1046–1047, 1994.
[14] G. Rubin, C. Beaulieu, V. Argiro, H. Ringl, A. Norbash, J. Feller, M. Dake, R. Jeffrey, and S. Napel, "Perspective volume rendering of CT and MR images: Applications for endoscopic imaging," *Radiology*, vol. 199, pp. 321–330, 1996.
[15] B. Simons, A. Morrison, R. Lev, and W. Verhoek-Oftendahl, "Relationship of polyps to cancer of the large intestine," *J. National Cancer Inst.*, vol. 84, pp. 962–966, 1992.
[16] N. V. Smirnov, "On the estimation of discrepancy between empirical curves of distribution for two independent samples" (in Russian), *Bull. Moscow Univ.*, vol. 2, pp. 3–16, 1939.
[17] P. Sprent, *Applied Nonparampetric Statistical Methods*, 2nd ed. London, U.K.: Chapman & Hall, 1993.
[18] D. J. Vining, D. Gelfand, R. Bechtold, E. Scharling, E. F. Grishaw, and R. Shifirin, "Technical feasibility of colon imaging with helical CT and virtual reality," in *1994 Ann. Meeting Amer. Roentgen Ray. Soc.*, New Orleans, p. 104.
[19] J. Zhang, J. W. Modestino, and D. A. Langan, "Maximum-likelihood parameter estimation for unsupervised stochastic model-based image segmentation," *IEEE Trans. Image Processing*, vol. 3, pp. 404–420, 1994.
[20] "Cancer facts and figures," Amer. Cancer Soc., Atlanta, GA, pt. 2, 1998.